

# Characterization and in vitro evaluation of electrospun chitosan/polycaprolactone blend fibrous mat for skin tissue engineering

Tilak Prasad · E. A. Shabeena · D. Vinod ·  
T. V. Kumary · P. R. Anil Kumar

Received: 21 May 2014 / Accepted: 3 August 2014 / Published online: 13 January 2015  
© Springer Science+Business Media New York 2014

**Abstract** The electrospinning technique allows engineering biomimetic scaffolds within micro to nanoscale range mimicking natural extracellular matrix (ECM). Chitosan (CS) and polycaprolactone (PCL) were dissolved in a modified solvent mixture consisting of formic acid and acetone (3:7) and mixed in different weight ratios to get chitosan-polycaprolactone [CS-PCL] blend solutions. The CS-PCL blend polymer was electrospun in the same solvent system and compared with PCL. The physicochemical characterization of the electrospun fibrous mats was done using scanning electron microscopy (SEM), Fourier transform infrared spectroscopy (FTIR), tensile test, swelling properties, water contact angle (WCA) analysis, surface profilometry and thermo gravimetric analysis (TGA). The CS-PCL fibrous mat showed decreased hydrophobicity. The CS-PCL mats also showed improved swelling property, tensile strength, thermal stability and surface roughness. The cytocompatibility of the CS-PCL and PCL fibrous mats were examined using mouse fibroblast (L-929) cell line by direct contact and cellular activity with extract of materials confirmed non-cytotoxic nature. The potential of CS-PCL and PCL fibrous mats as skin tissue engineering scaffolds were assessed by cell adhesion, viability, proliferation and actin distribution using human keratinocytes (HaCaT) and L-929 cell lines. Results indicate that CS-PCL is a better scaffold for attachment and proliferation of keratinocytes and is a potential material for skin tissue engineering.

## 1 Introduction

Tissue engineering has emerged as a promising solution in treating extensive loss/damage of skin caused by burns, trauma and diseases. Critical determinants in favorable wound healing outcomes are largely based on the physicochemical nature of scaffolds, cell types and cell material interactions [1]. Biodegradable natural and synthetic polymers with favorable mechanical properties and degradation kinetics are extensively explored for therapeutic applications [2]. Electrospinning is an efficient method for the fabrication of biomimetic scaffolds with micro to nano scale topography mimicking natural extracellular matrix (ECM) for favorable cell attachment and proliferation [3].

Polycaprolactone (PCL) is a semi-crystalline, synthetic polymer, extensively used for biomedical applications due to its properties like low melting point, high tensile strength, non-toxic nature and biodegradability [4]. PCL has been investigated as potential matrix for skin tissue engineering [5]. However use of PCL as such in tissue engineering is limited due to its poor bioregulatory activity, high hydrophobicity, lack of functional groups and neutral charge. Various physico-chemical and post-processing surface modification techniques have been reported to overcome these limitations [6]. Blending another polymer with desired characteristics will enable to bring down the disadvantages of PCL [7]. Chitosan [(1–4)-linked 2-amino-2-deoxy-D-glucopyranose], a natural polymer derived from chitin has been widely used in biomedical applications due to its key advantages like biocompatibility, presence of functional groups and high hydrophilicity [8, 9]. Chitosan (CS) is extensively used for wound healing applications and for skin tissue engineering in combination with other biopolymers [10, 11]. Blending CS with PCL is one of the easy approaches to bring desired physico-chemical

T. Prasad · E. A. Shabeena · D. Vinod ·  
T. V. Kumary · P. R. Anil Kumar (✉)  
Tissue Culture Laboratory, Biomedical Technology Wing, Sree  
Chitra Tirunal Institute for Medical Sciences and Technology,  
Poojappura, Thiruvananthapuram 695012, Kerala, India  
e-mail: pranilkumar@yahoo.com; anilkumarpr@sctimst.ac.in

characteristics by combining the properties of both the polymers [12]. However, low solubility, higher surface tension, inherent poor processibility, and reduced spinnability of CS restrict its use in electrospinning [13]. Different solvent systems including dilute hydrochloric acid, acetic acid, neat formic acid, dichloroacetic acid and trifluoroacetic acid has been experimented to study the electrospinning of CS [14]. The difficulty in electrospinning of the CS can be overcome by blending with fiber-forming polymers such as poly (ethylene oxide), poly (vinyl alcohol), PCL etc. Blending CS with PCL will give micro to nano scale fibrous scaffolds that serves like ECM for favorable cell attachment and proliferation. A recent report on formic acid and acetone mixture as single solvent for PCL and CS showed better spinnability [15].

In this study, chitosan-polycaprolactone (CS-PCL) blend was prepared in a modified single solvent mixture consisting of formic acid and acetone and subsequently electrospun to fabricate fibrous mats. The CS-PCL fibrous mats were characterized and evaluated *in vitro* using human keratinocytes (HaCaT) for skin tissue engineering

## 2 Materials and methods

### 2.1 Materials

Polycaprolactone (MW 70,000–80,000), Fluorescein diacetate (FDA) and Rhodamine-phalloidin was purchased from Sigma, USA. CS from shrimp shells (degree of deacetylation < 90 %), propidium iodide (PI), Rhodamine B and Fluorescein were purchased from Hi Media; India. Formic acid and acetone were purchased from SD fine chemicals, India; Syringes and needles were purchased from BD biosciences Ltd, Spain. Minimum essential medium (MEM), Penicillin–Streptomycin (Pen Strep—10,000 U/ml), fetal bovine serum (FBS) were from Gibco, Invitrogen, India. Mouse subcutaneous fibroblast cell line (L-929) and HaCaT, were procured from National Center for Cell Sciences, Pune, India.

### 2.2 Preparation of polymer solutions

The solvent was prepared by mixing formic acid and acetone at volume ratio of 3:7 respectively. This solvent was used to prepare 2 % CS and 10 % PCL solutions by overnight stirring. The CS-PCL blend solution was then prepared by mixing the above solutions overnight at CS:PCL ratio of 4:6 and 2:8.

In order to differentiate the PCL and CS fibers in electrospun mat, the PCL and CS polymers were separately tagged with Fluorescein and Rhodamine B respectively to a final concentration of 1.5  $\mu\text{g/ml}$ . The tagged CS-PCL blend polymer solution was prepared as described above.

### 2.3 Electrospinning

The PCL and CS-PCL solutions were electrospun in a horizontal spinning configuration, using a customized electrospinning unit (Holmarc Optomechatronics Pvt Ltd, India). Polymer solutions were supplied continuously to a syringe connected to a 21 gauge blunt end needle with a feeding rate of 1 ml/h for 72 h. A high voltage of 16 kV was applied between the needle kept at a distance of 20 cm from rotating mandrel set at 200 revolutions per minute. The fibrous mats were detached from mandrel, rinsed twice in deionized water to remove the solvent and air dried at 37 °C overnight. The scaffolds were sterilized by exposing to UV for 30 min prior to cell culture studies. The CS-PCL fibrous mats were compared with PCL mats.

In order to differentiate the presence of PCL and CS in the electrospun CS-PCL mat the fluorescent tagged blend polymers was electrospun on to a clean glass slide placed on grounded collector as described above and analyzed under Laser Scanning Confocal Microscope (LSM 510 meta, Carl Zeiss, Germany)

### 2.4 Characterization of electrospun scaffolds

Physico-chemical properties of scaffolds were characterized using scanning electron microscopy (SEM), surface profilometry, water contact angle and thermo gravimetric analysis (TGA).

#### 2.4.1 Morphology analysis

The morphology and structural details of fibrous mats was analyzed using SEM (Hitachi S2500, Japan). The PCL and CS-PCL were coated with gold in a sputter coating device and observed under SEM. The digital images from randomly selected areas were imported to NIH Image-J software to analyze the fiber diameter. The size distribution of PCL and CS-PCL fibrous mat was plotted in Microsoft Excel.

#### 2.4.2 Fourier transform infra-red spectroscopy (FTIR)

The surface analysis of PCL and CS-PCL blend fibrous mats were evaluated by FTIR spectroscopy (Jasco 6300, USA) in the range 4,000–400  $\text{cm}^{-1}$ . CS in powder form was also analyzed by KBr pellet method.

#### 2.4.3 Swelling test

The swelling property of the PCL and CS-PCL blend fibrous mat were analyzed in phosphate buffered saline (PBS) for 80 min. Dry samples ( $W_d$ ) were weighed and

immersed in PBS. The samples were taken at specific time intervals and excess water was blotted out before obtaining the wet weight ( $W_s$ ). The percentage swelling ratio was calculated using the equation

$$Q = \frac{W_s - W_d}{W_d} \times 100$$

#### 2.4.4 Tensile strength

The tensile strength of CS-PCL and PCL fibrous mats were evaluated using a Instron Universal Materials Testing Machine (Instron Corp., India). Rectangular strips of  $1 \times 5$  cm PCL and CS-PCL fibrous mats having thickness ranging from 0.189 to 0.214 mm was used for analysis at a crosshead speed of 10 mm/min ( $n = 4$ ). To compare the mechanical properties of fibrous mat with skin tissue, murin skin having the same dimension with thickness of 0.22 mm was used.

#### 2.4.5 Water Contact angle

The wettability of the electrospun fibrous mats of PCL and CS-PCL were measured at room temperature in a goniometer (Data Physics OCA 15 plus, Germany) by sessile drop method. Water drops of 5  $\mu$ l were placed at multiple locations of triplicate samples and the contact angle was recorded.

#### 2.4.6 Surface profilometry

The surface roughness of PCL and CS-PCL fibrous mats were qualitatively evaluated with a noncontact scanning topography instrument—Talysurf CLI 1000 (Taylor Hobson) equipped with Talymap Gold 4.1 analysis software. Sample was fixed on a flat surface and 40 line profiles were obtained overlapping the edge and the surface using a chromatic length aberration gauge. Three-dimensional images were constructed and root mean square value (Ra) of roughness was calculated.

#### 2.4.7 Thermo gravimetric analysis (TGA)

Thermal degradation of pure CS, electrospun fibrous mats of PCL and CS-PCL were analyzed by simultaneous DSC-TGA thermogravimetric analyzer (SDT Q600, TA Instruments Inc., USA). The samples were pre weighed (15 mg) and TGA was performed between 20 and 600 °C at a programmed heating rate of 10 °C/min.

### 2.5 Cell culture studies

General cytotoxicity of scaffolds was carried out using L-929 cells and specific cytocompatibility was assessed

using HaCaT cells. Both the cell lines were maintained in MEM supplemented with 5 % FBS and  $1 \times$  PenStrep at 37 °C in a CO<sub>2</sub> incubator set at 95 % relative humidity and 5 % CO<sub>2</sub>. Confluent cultures were treated using Trypsin—EDTA and cell suspension was counted in haemocytometer prior to cell seeding. Cytotoxicity was evaluated by direct contact and test on extract method. Cytocompatibility and suitability of CS-PCL scaffolds for skin tissue engineering were analyzed by evaluating cell adhesion, distribution of actin cytoskeletal filaments, cell viability and proliferation.

#### 2.5.1 Cytotoxicity by direct contact

The cytotoxicity of PCL and CS-PCL electrospun fibers were tested by direct contact method (ISO10993-5). High-density polyethylene and copper discs were used as negative and positive controls respectively. Approximately  $3 \times 10^4$  cells were seeded per well of 24 well plate and maintained until subconfluency in a CO<sub>2</sub> incubator. The culture medium was removed and PCL and CS-PCL of size  $4 \times 4$  mm was carefully placed on the cell monolayer. Sufficient culture medium was added and cells were incubated for 24 h. Cytotoxicity was assessed by monitoring the morphology, cell detachment, cell lysis and vacuolization of the cells under an inverted phase contrast microscope (Motic, Hong Kong). The viability of cells after direct contact test was also determined by incubating with 0.5 mg/ml neutral red for 10 min and observed under inverted microscope using bright field mode.

#### 2.5.2 Cytotoxicity by test on extract

Extracts of PCL and CS-PCL were obtained by incubating the scaffolds with  $20 \times 20$  mm size in 1 ml MEM containing FBS for 24 h at 37 °C with continuous shaking. Extract was added to subconfluent L-929 cells and incubated at 37 °C for 24 h. Cells cultured in normal medium were taken as cell control. After removing extract and medium, 100  $\mu$ l MTT reagent (0.5 mg/ml in serum free medium) was added and incubated for 2 h at 37 °C in a CO<sub>2</sub> incubator to allow the formation of formazan crystals. The formazan product formed was dissolved in isopropanol and absorbance was taken at 570 nm in a multiwell plate reader (Biotek Powerwave XS, USA).

#### 2.5.3 Cell adhesion and viability on fibrous mats

Cell adhesion and viability of cells on PCL and CS-PCL fibrous scaffold were analyzed using L-929 and HaCaT cells. Samples having  $1 \times 1$  cm size were preconditioned with culture medium for 15 min and then transferred to a fresh cell culture dish. L-929 and HaCaT cells were transferred to preconditioned scaffolds at a concentration of  $1 \times 10^5$  cells/100  $\mu$ l and incubated inside CO<sub>2</sub>

incubator for 20 min to allow cells to adhere. Additional 1 ml of culture medium was supplemented and cell seeded scaffolds were further incubated for 4 days.

The cell adhesion on electrospun scaffolds were analyzed by SEM. After 4 days in culture the cell seeded samples were fixed in 3.5 % glutaraldehyde overnight and washed twice with 0.1 M PBS. The samples were dehydrated in ascending grades of alcohol and critical point dried (Hitachi, HCP-2), and sputter coated with gold using an ion sputter device (Hitachi, E 101) prior to imaging under SEM (Hitachi S2500).

The viability of cells adhered on PCL and CS-PCL for 48 h were analyzed by FDA (live) and PI (dead) staining. The cell seeded samples were incubated with 1 ml FDA medium (10  $\mu\text{g/ml}$  in serum free MEM) for 15 min followed by addition of 100  $\mu\text{l}$  of PI (5  $\mu\text{g/ml}$  in PBS). Cells were further incubated for 30 s and examined under a fluorescence microscope [Leica DMI 6000B equipped with I3 (green) and N21 (red) filter].

#### 2.5.4 Cytoskeletal staining

The cytoskeletal organisation was analysed by staining actin microfilaments using rhodamine tagged phalloidin. L-929 and HaCaT cells were cultured on PCL and CS-PCL as described before for 48 h were fixed in 4 % paraformaldehyde for 1 h. Cells were rinsed with PBS and permeabilized with 0.1 % PBS- Triton-X 100 for 1 min. Rinsed cells were incubated with rhodamine-phalloidin for 15 min. The fluorescence was observed under fluorescence microscope using red filter (N21) [Leica DMI 6000].

#### 2.5.5 Cell proliferation on scaffold

UV sterilized and preconditioned scaffolds of size  $1 \times 1$  cm were seeded with approximately  $1 \times 10^6$  cells. The cellular activity was estimated by MTT assay at the end of 2 and 4 days as described before. The significance was calculated by students *t* test.

### 3 Results

#### 3.1 Fabrication of electrospun fibrous mats

The PCL and CS-PCL blend solutions were electrospun to get microfibrillar mats. The effect of the blending concentration in fiber formation was determined at different weight ratios of CS with PCL (4:6 and 2:8).

#### 3.2 Scanning electron microscopy

The CS-PCL blend fibrous mat was compared with PCL mat. The PCL mats obtained from the formic acid:acetone

solvent showed very fine and dense fibers (Fig. 1a). The CS-PCL fibrous mats at weight ratio of 4:6 showed extensive bead formation (data not shown). The fibrous mats at 2:8 CS and PCL weight ratio formed homogeneous fibers without bead formation. (Fig. 1b). A marked reduction in fiber density and increase in fiber diameter was noted in CS-PCL scaffolds. The fiber size distribution measured by image analysis of PCL and CS-PCL showed variations in the fiber diameter in the range 0.5–2.0  $\mu\text{m}$  (Fig. 1c).

#### 3.3 Laser scanning confocal microscopy

In order to determine the presence of both the polymers in the electrospun CS-PCL fibrous mats the polymers were tagged with different fluorochromes. Confocal analysis showed the presence of both fibers in the CS-PCL fibrous mats with CS-expressing red and PCL green fluorescence (Fig. 2). The intensity profile was plotted to further confirm the results. The plot showed more green fibers corresponding to PCL along with some red fibers (CS). Some fibers coexpressing both the fluorochromes were noted.

#### 3.4 Spectroscopic analysis

The IR spectral analysis of CS-PCL was carried out and compared with that of PCL mat and CS powder (Fig. 3). The CS showed characteristic peaks at  $3,431\text{ cm}^{-1}$  for N–H and O–H stretching and peak at  $2,877\text{ cm}^{-1}$  from asymmetric bending of C–H group. The spectrum of PCL showed peaks at  $1,720\text{ cm}^{-1}$  and  $2,919\text{ cm}^{-1}$  for ester carbonyl group and C–H respectively. However the O–H stretching peak for CS at  $3,431\text{ cm}^{-1}$  in the CS-PCL scaffold was flattened.

#### 3.5 Swelling test

The CS-PCL blend fibrous mats prepared in formic acid–acetone solvent showed improved hydration compared to PCL mats (Fig. 4). The percentage swelling ratio of CS-PCL in PBS at 10 min was 20 % where as PCL showed only 15 %. The CS-PCL fibrous showed maximum swelling ratio within initial 40 min whereas the PCL showed very minimal steady swelling. The CS-PCL swelling increased to 146 % over 80 min when PCL fibrous mat could swell only up to 46 %.

#### 3.6 Tensile strength

The tensile properties of electrospun CS-PCL fibrous mats measured and compared with that of PCL mats and murine skin. The maximum percentage strain expressed by CS-PCL was lower (26.73 %) compared to that of PCL



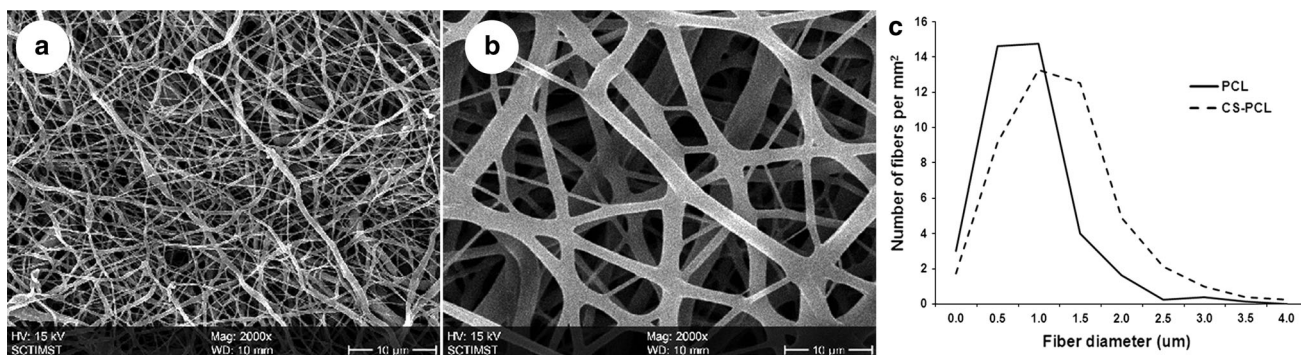


**Fig. 1** SEM micrographs showing electrospun fibrous mats **a** PCL and **b** CS-PCL at 2:8 weight ratios **c** Fiber size distribution of PCL and CS-PCL

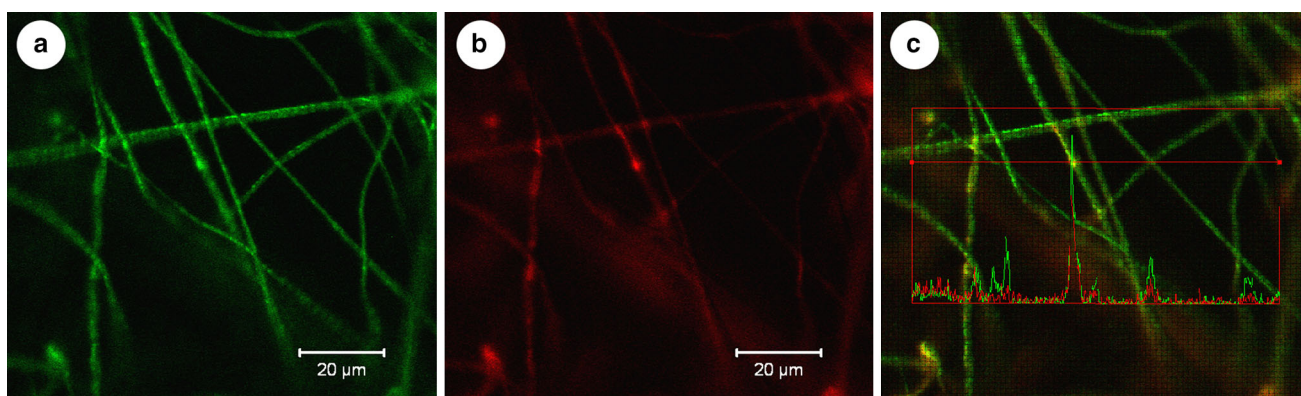


**Fig. 2** Confocal micrograph of fluorochrome labeled electrospun CS-PCL mat. **a** PCL fibers expressing fluorescein **b** CS fibers expressing Rhodamine and **c** intensity analysis of the merged image of **a** and **b**

(84.14 %) due to decrease in elasticity. However the Young's modulus of CS-PCL (12.41 MPa) was increased compared to PCL (3.94 MPa). This confirms the remarkable improvement of mechanical property of CS-PCL blend fibrous mats with respect to PCL alone. Additionally the CS-PCL showed 66.6 % of tensile property of murin skin tissue (18.20 MPa).

### 3.7 Contact angle

The PCL fibrous mat showed water contact angle of  $127 \pm 5.2^\circ$ , where as CS-PCL blend fibrous mat expressed lower values of  $117 \pm 4.9^\circ$ . This confirms that CS-PCL mats is relatively more hydrophilic compared to that of PCL.

### 3.8 Surface profilometry

The surface roughness and thickness of ES mats of PCL and CS-PCL were qualitatively evaluated by light profilometry. The CS-PCL showed improved surface roughness compared to PCL mats. The roughness average ( $R_a$ ) of

electrospun fibrous mats estimated by profilometry where  $R_a = 0.315 \pm 0.0280$  for PCL and  $R_a = 0.549 \pm 0.022$  for CS-PCL. The thickness estimated by line profile analysis was 100 and 90 µm for PCL and CS-PCL respectively.

### 3.9 Thermo gravimetric analysis

The thermal analysis of CS-PCL fibrous mats showed an increased decomposition temperature 275–350 °C compared to PCL mats (250–300 °C) (Fig. 5a). The degradation of pure CS was also compared with PCL and CS-PCL degradation curves. CS has comparatively lower decomposition temperature of 175–225 °C. To resolve the presence of CS in the CS-PCL blend a derivative weight loss was plotted from the TG data (Fig. 5b). The DTG of CS-PCL showed minor peak corresponding to weight loss of CS at 233–320 °C and an intense peak of PCL at 325–425 °C. An increase in the melting temperature was noted for the CS-PCL blend. These results indicate the successful blending of CS with PCL. The

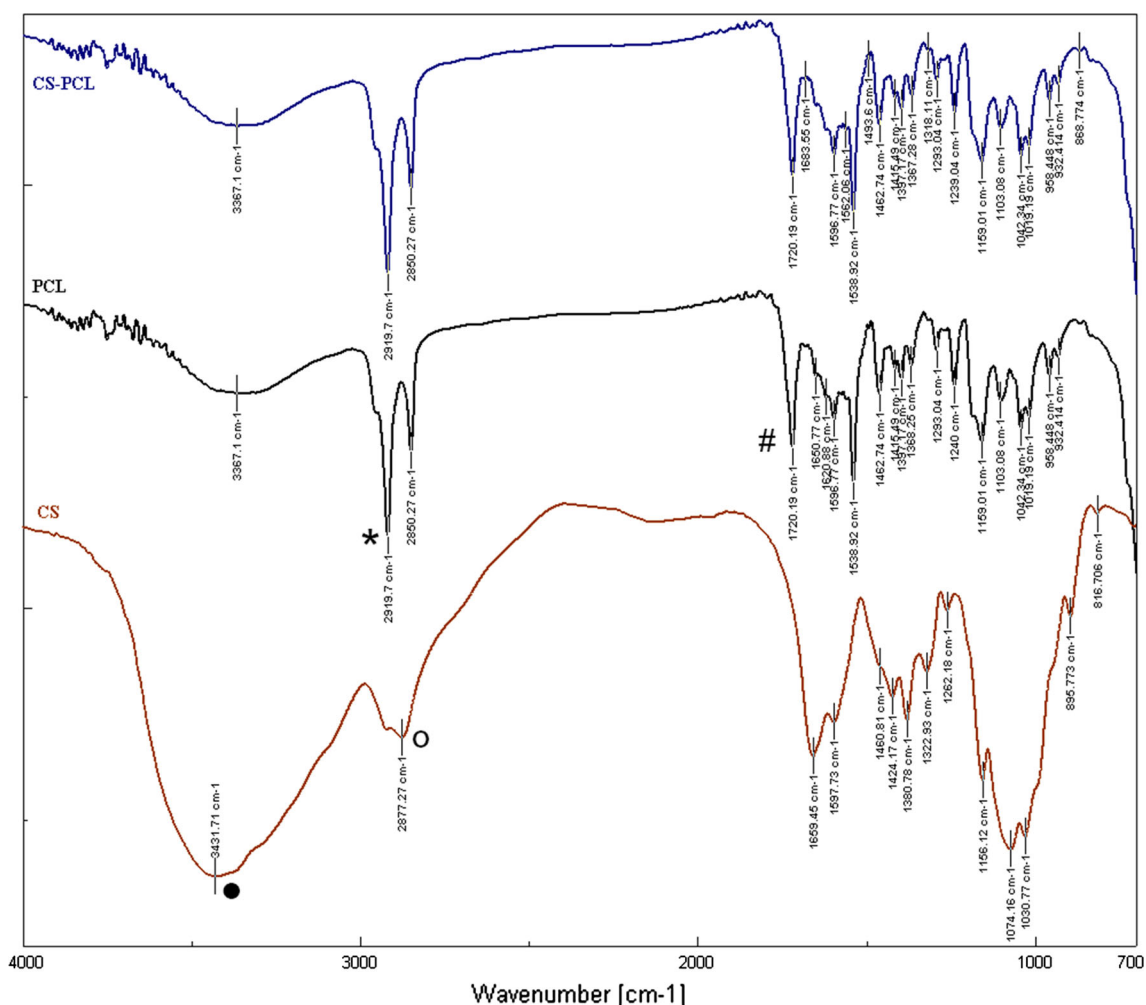


**Fig. 3** FTIR spectrum of PCL, CS-PCL and CS. The peaks of CS at  $3,431\text{ cm}^{-1}$  (●) and  $2,877\text{ cm}^{-1}$  (○) were flattened in CS-PCL mats. The characteristic peaks of PCL at  $1,720\text{ cm}^{-1}$  (#) and  $2,919\text{ cm}^{-1}$  (\*) were present in both PCL and CS-PCL fibrous mats

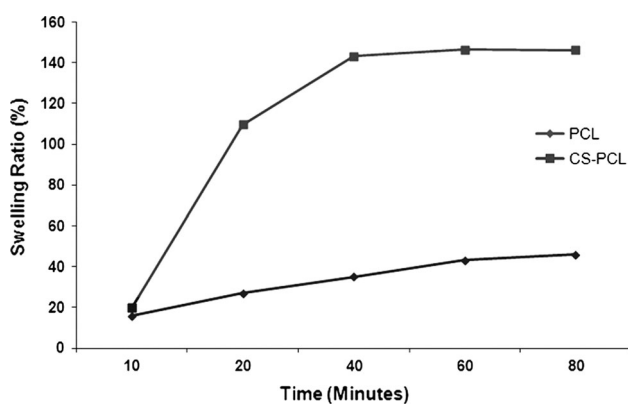


**Fig. 4** Swelling properties of PCL and CS-PCL fibrous mats ( $n = 4$ )

weak intensity of CS peak in the blend CS-PCL mats is attributed to the lower concentration of CS after electrospinning.

### 3.10 In vitro cell culture studies

Three dimensional scaffolds with biomaterials and cells address the shortage of tissues and organs for transplantation and repair in tissue engineering. The scaffolds for cell growth should be porous with adequate surface chemistry and biocompatibility [16]. In the present study fibrous mats were evaluated in vitro by direct contact and test on extract method.

#### 3.10.1 Cytotoxicity by analysis

Cytotoxicity test by direct contact method revealed the response of cells towards test materials when both are in contact. The PCL and CS-PCL scaffolds in direct contact with L-929 fibroblast monolayer for 24 h showed non-cytotoxicity. The toxic responses like cell detachment, lysis and extensive vacuolization were absent (Fig. 6a–b). This was further confirmed by analyzing the viability by neutral red staining (Fig. 6c–d).

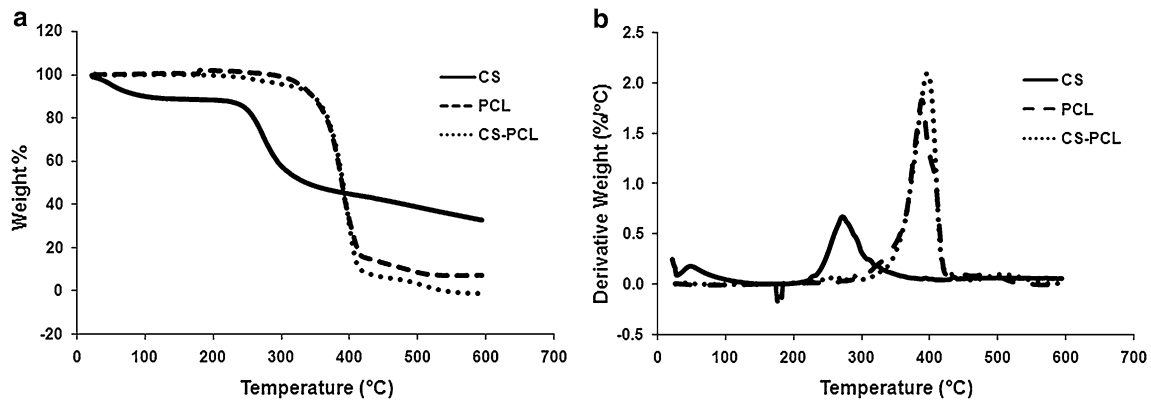


**Fig. 5** Thermal analysis: **a** TG of CS, CS-PCL and PCL, **b** DTG of CS, CS-PCL and PCL

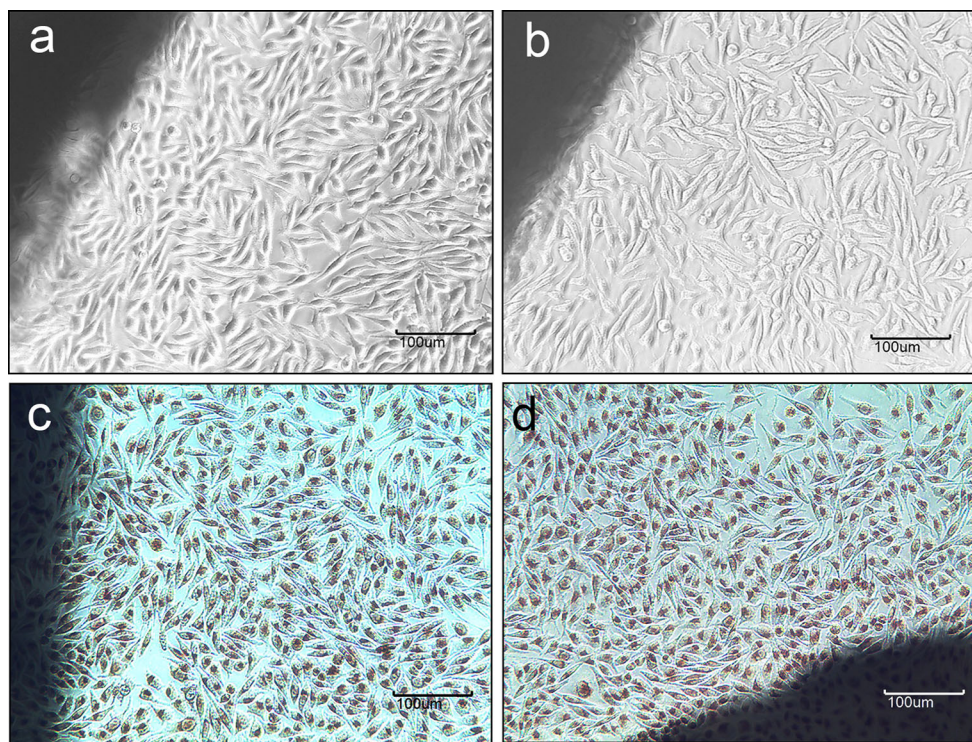


**Fig. 6** Direct contact cytotoxicity test showing non cytotoxicity of **a** PCL and **b** CS-PCL. The viable cells around **c** PCL and **d** CS-PCL showing neutral red uptake

### 3.10.2 Cytotoxicity by test on extract

The possible toxicity from the leachants from biomaterials can be quantitatively evaluated by MTT assay of cells exposed to material extract. Metabolic activity was calculated by considering the cell control as 100 %. L-929 fibroblast cells exposed to the extracts of PCL showed  $95.2 \pm 4.8$  % and CS-PCL showed  $100 \pm 4.6$  % (Fig. 7).

### 3.10.3 Cell adhesion and viability

We propose the CS-PCL fibrous mat for skin tissue engineering applications and hence the fibrous mats were evaluated for its suitability with human epidermal keratinocytes (HaCaT) in addition to mouse fibroblast (L-929) cell lines. The L-929 and HaCaT cells on CS-PCL fibrous mats showed good attachment, spreading with characteristic morphology and integration with CS-PCL fibers (Fig. 8).



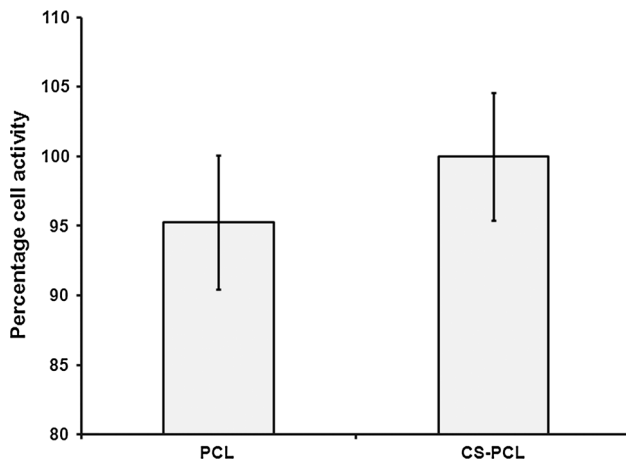


**Fig. 7** Percentage cell activity of L-929 cells exposed to extracts of PCL and CS-PCL calculated from cell control ( $n = 5$ )

The cells on PCL mats appeared more round in shape. The L-929 cells on CS-PCL observed under high magnification revealed better cell integration with fibrous mats compared to cells on PCL. The keratinocytes on PCL

expressed good cell–cell contact with no exposed fibers whereas the cells on CS-PCL showed cell–cell contact as well as integration with fibrous mats (Fig. 9). This is required for skin tissue engineering as keratinocytes need good cell–cell contact and strong cell ECM interaction.

Viability of cells adhered on CS-PCL and PCL fibrous mats were visualized by live dead staining using FDA and PI. The result showed that both L-929 and HaCaT cells adhered on the fibrous mats were viable (Fig. 10). HaCaT cells expressed patched cell growth on PCL and CS-PCL. Additionally the colonies formed on CS-PCL were comparatively large which could be due to combined property of PCL and CS.

#### 3.10.4 Cytoskeletal staining

The L-929 and HaCaT cells on PCL and CS-PCL showed characteristic morphology with cortical staining pattern (Fig. 11). L-929 cells adhered and spread similarly on PCL and CS-PCL where as HaCaT cells showed extensive patch formation and characteristic polygonal morphology on CS-PCL.

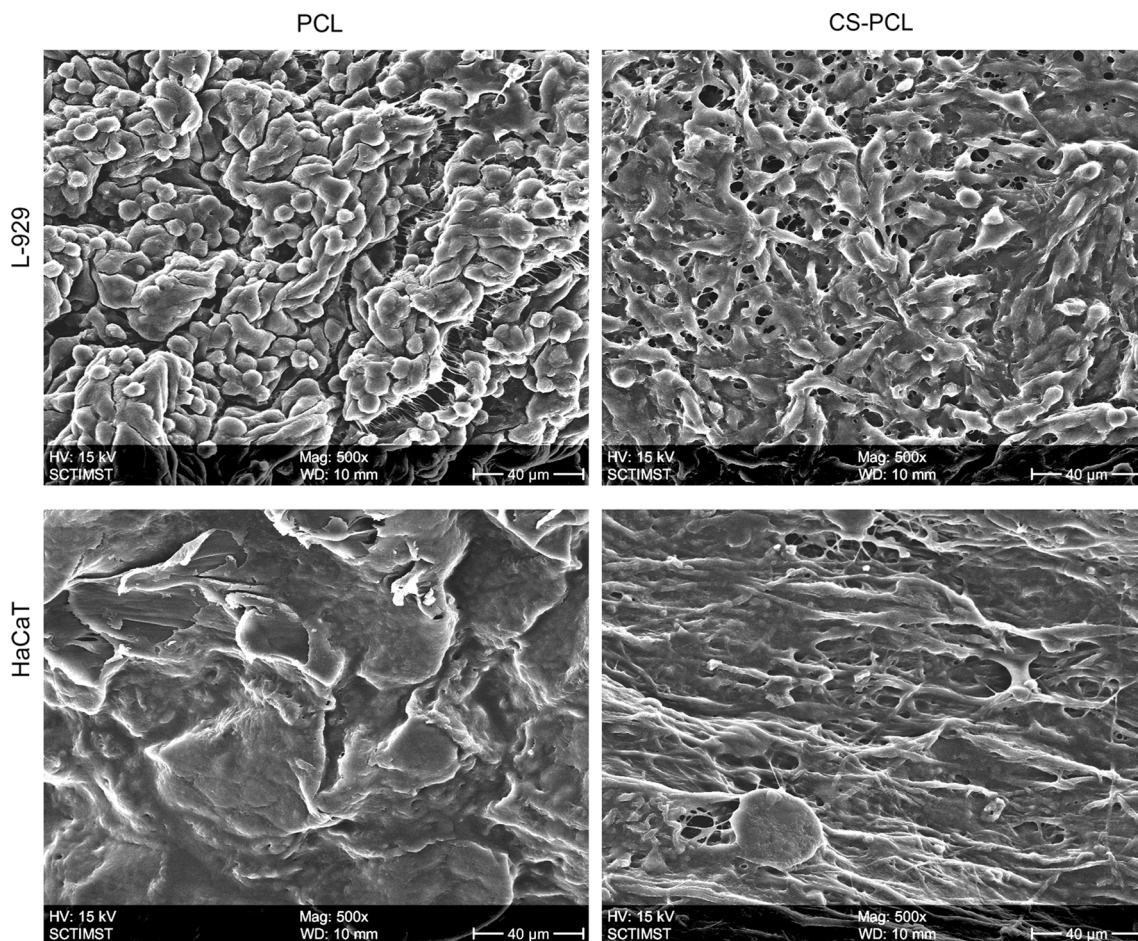


**Fig. 8** SEM images showing L-929 and HaCaT cell adhesion on PCL and CS-PCL fibrous mats. The L-929 cells seeded on PCL were more round than cells on CS-PCL, whereas the HaCaT cells formed sheets over both fibrous mats

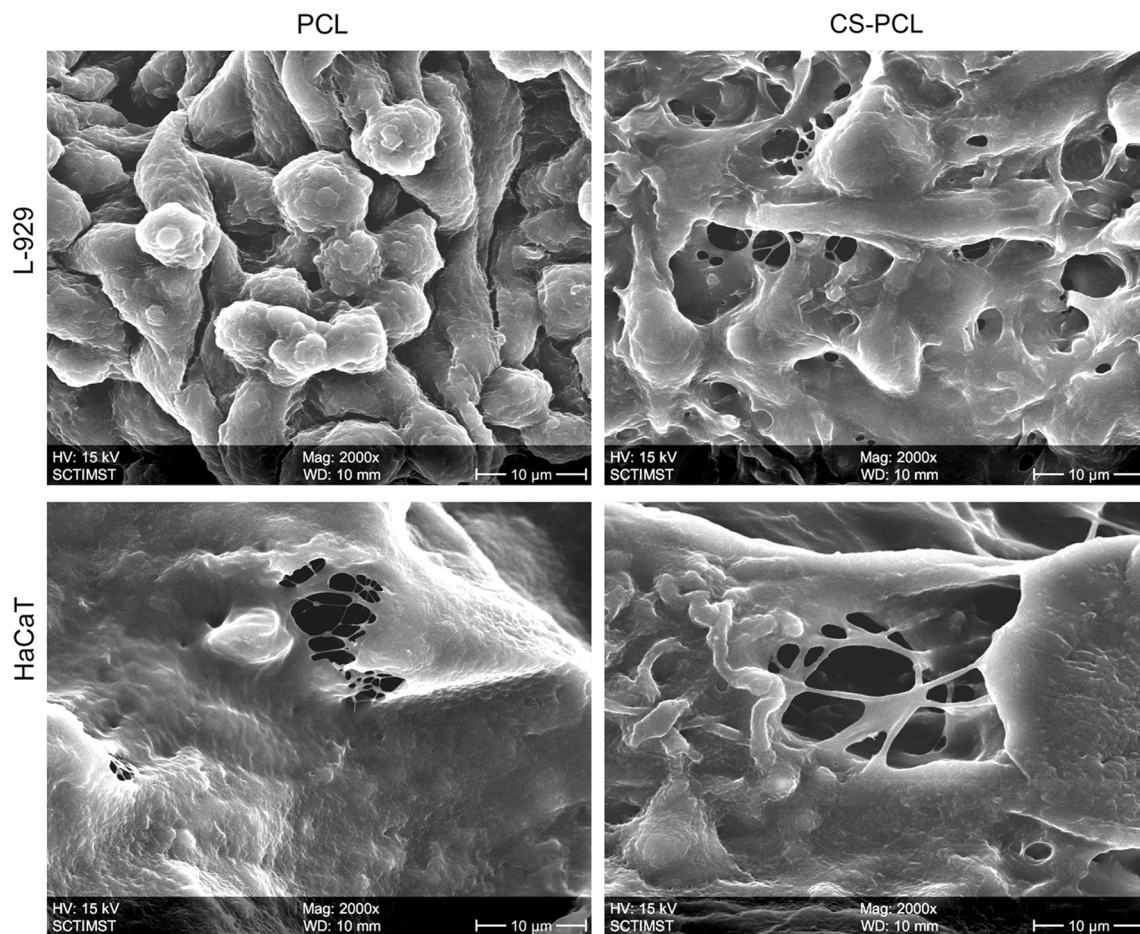


**Fig. 9** High magnification SEM images of Fig. 8 showing L-929 and HaCaT cells on PCL and CS-PCL fibrous mats. CS-PCL showed better support for cell cell and cell-material interaction

### 3.10.5 Cell proliferation on scaffold

Proliferation of L-929 cells on CS-PCL fibrous mats was evaluated by MTT assay and compared with PCL (Fig. 12). The cell growth on CS-PCL measured at two time points were significantly more compared to PCL.

## 4 Discussion

Electrospun nanofiber mats are widely used in tissue engineering as scaffolds in biological substitutes [17]. PCL is one of the biodegradable poly ester approved by Food and Drug Administration (FDA), which has been used in biomedical applications [18]. However, PCL scaffolds have not hitherto been used for cell culture applications involving tissue engineering due to its high hydrophobicity and poor cell adhesion. The individual problems associated with PCL and CS can be limited by preparing graft polymers, blends and composites [7, 12, 19]. Blending PCL with other synthetic/natural polymers is a simple approach

to bring desired mechanical and biological properties. CS is a natural polymer well known as a biomaterial due to its key properties like non toxicity, non immunogenicity, solubilization in most acids [20] and has been used as a matrix for tissue engineering approaches involving skin, bone, cartilage, liver and blood vessel regeneration [21]. The electrospinning of PCL and CS has been extensively studied as scaffolds for tissue engineering.

Electrospinning of CS is possible in acids and organic solvents such as trifluoroacetic acid (TFA), glacial acetic acid and dichloromethane (DCM). Rigorous conditions of 7 % concentration in 90 % acid solution and 4 kV/cm electric field is required for electrospinning deacetylated CS [22]. Electrospinning of pure CS in acid solution results in bead formation and non continuous fibers [23]. The electrospinnability of CS can be improved by in TFA and DCM but the degradation and fibrous nature are affected in neutral or weak solutions [24]. Here we report a hybrid fibrous polymer mat for skin tissue engineering which comprises of CS and PCL, fabricated in a modified single solvent system of formic acid and acetone. Various parameters such as



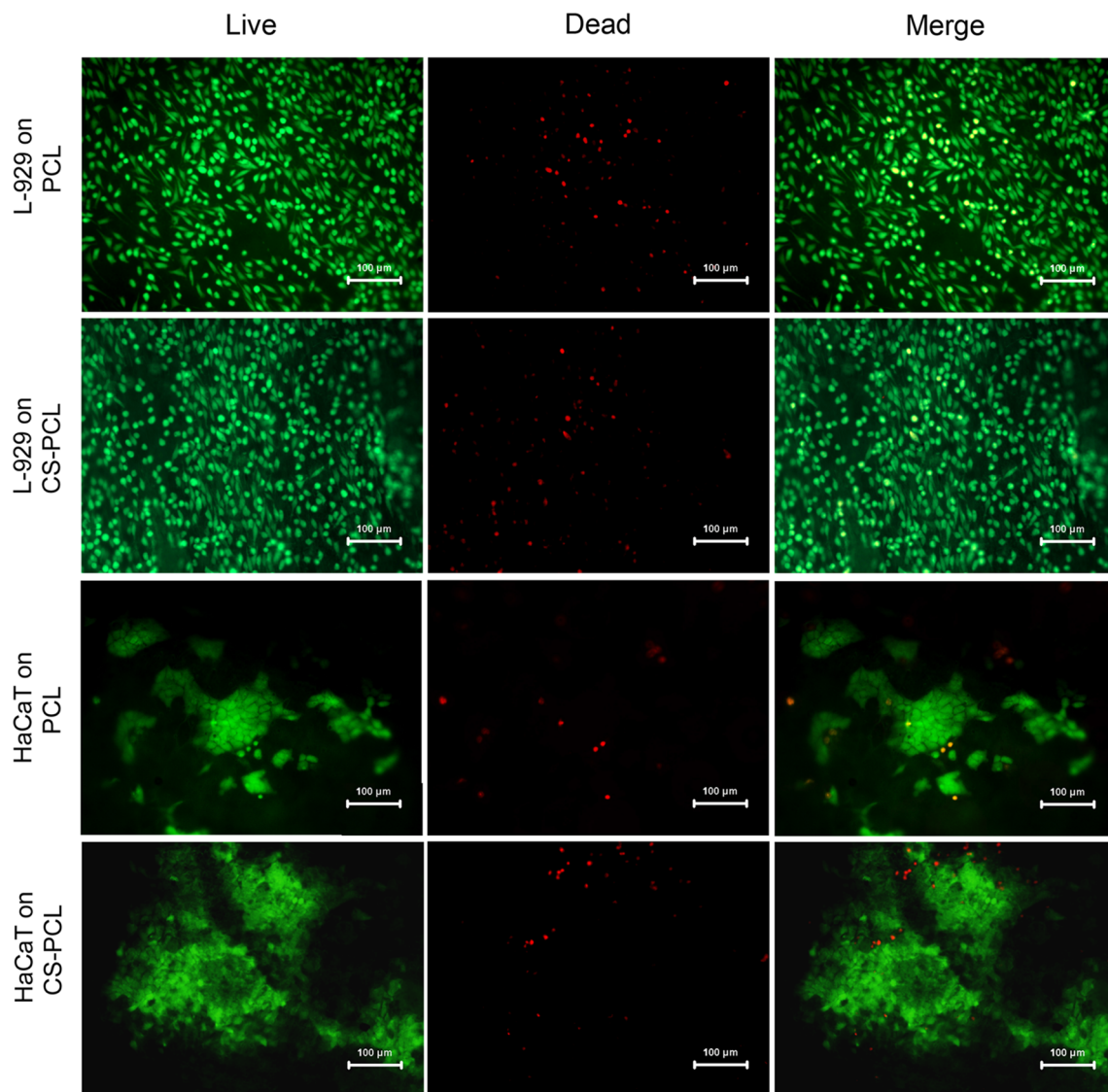


**Fig. 10** Live dead staining of L-929 and HaCaT cells cultured on PCL and CS-PCL fibrous mat The *first lane* shows live cells (*green*), *second lane* represent dead cells (*red*) and *third lane* is the merge of live and dead (Color figure online)

applied voltage, tip to collector distance, viscosity and concentration of solution can influence the morphology of fibers formed by electrospinning [25]. Here an optimal formic acid:acetone ratio and electrospinning conditions were further optimized from previous report [15]. The conditions of electrospinning of blend CS-PCL solution yielded bead free fibers at flow rate of 1 ml/h, on a mandrel kept at a distance of 20 cm, rotating at 200 rpm within a potential difference of 16 kV. Since PCL is a versatile polymer with good electrospinnability the CS-PCL blend fibers were compared with PCL fibers. The morphology of CS-PCL and PCL under SEM showed bead free architecture with the fiber diameter in micron range. It is known that fiber diameters from nano to micron size influence the focal adhesion points and favour cell adhesion [26]. The spectral

analysis of the CS-PCL blend and PCL scaffolds and CS showed similarity with previous reports [15].

The spectral analysis of CS-PCL mat compared PCL mat and CS powder showed bulk characteristic of PCL from the peaks at  $1,720$  and  $2,919\text{ cm}^{-1}$  for ester carbonyl group and C-H respectively. The characteristic peaks of CS for N-H and O-H stretching at  $3,431\text{ cm}^{-1}$  and peak representing asymmetric bending of C-H group at  $2,877\text{ cm}^{-1}$  were absent in CS-PCL blend. This could be due to the lower concentration of CS compared to PCL in the blend fibrous mat. However, the presence of CS in the CS-PCL blend mats was confirmed by the fluorescence tagging and electrospinning of the scaffolds.

The cell adhesion, proliferation and differentiation on a polymer surface are affected by the wettability and surface



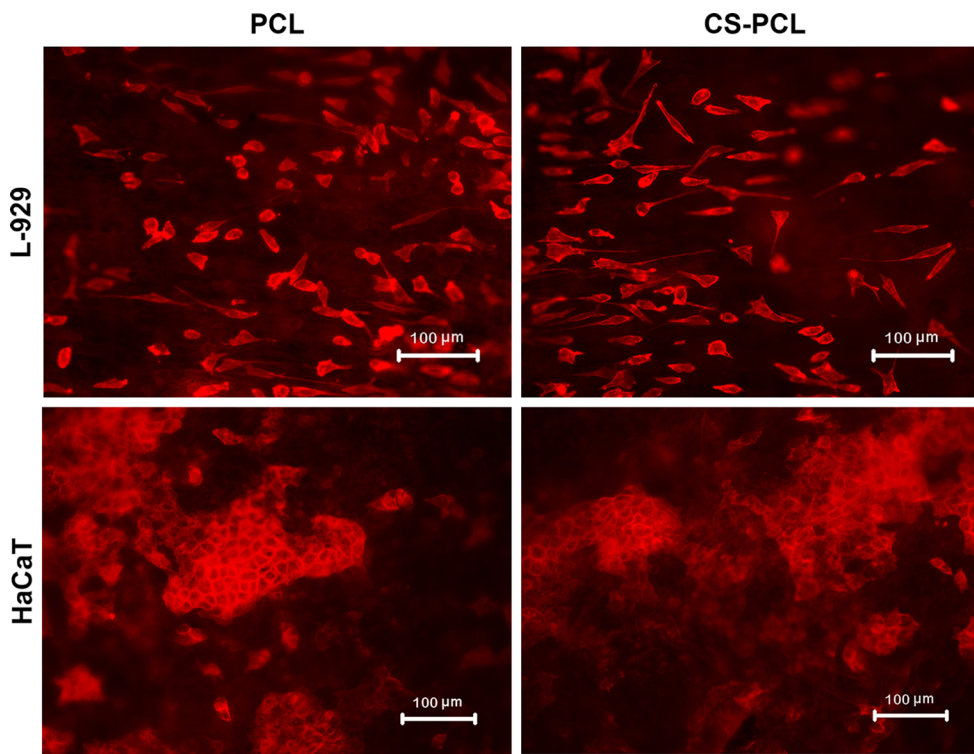


**Fig. 11** Actin filament distribution of L-929 and HaCaT cells on PCL and CS-PCL fibrous mat

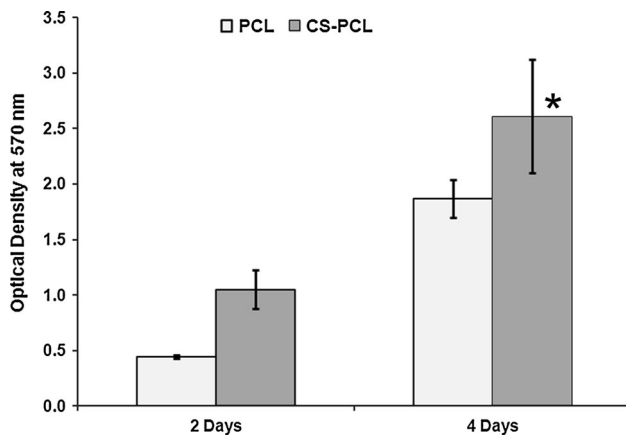


**Fig. 12** Cell proliferation by MTT assay of L-929 cells on PCL and CS-PCL. Cells proliferated more on CS-PCL compared to PCL. \* $P < 0.05$

roughness [27]. The physico chemical properties of CS-PCL blend scaffolds was further analyzed for its suitability for cell culture applications by analyzing the wettability, swelling characteristics and surface roughness. The swelling test gives an insight to the hydrated status of materials before and after cell seeding. The better hydration of CS-PCL fibrous mats relative to PCL alone is contributed by the presence of CS in the blend mat. The swelling characteristics of CS-PCL were similar to earlier reports of

Neves et al. prepared by wet spinning in formic acid as solvent [28]. The improved swelling behavior exhibited by the CS-PCL scaffolds could better help in tissue engineering application by influencing cell adhesion viz adsorption of proteins followed by cell adhesion on the adsorbed proteins [29, 30]. Light profilometry is a non destructive method to analyze thickness and surface morphology of electrospun membranes [31]. Profilometry analysis of CS-PCL scaffolds showed an improved surface roughness. The water contact angle analysis of CS-PCL showed reduced hydrophobicity. The reduction in hydrophobicity and increase in surface roughness indicates the successful blending of the CS and PCL. The increased surface roughness noted in CS-PCL scaffolds is desirable for in vitro cell culture as reported before [6]. Since the CS-PCL mats is proposed for skin tissue engineering, the tensile strength of the mats were compared with murine skin. The CS-PCL mats showed Young’s modulus comparable to murine skin. The scaffolds for tissue engineering should be porous with adequate surface chemistry and biocompatibility [32]. The biocompatibility of electrospun CS-PCL fibrous mats was evaluated in vitro by direct contact cytotoxicity, test on extract, cell adhesion, cell viability and proliferation. The cytotoxicity tests conducted on CS-PCL and PCL samples by directly exposing it to cells or its extract to cells, confirmed that the fibrous mats are non-cytotoxic. The morphological evaluation showed

no toxic response towards the samples. We propose the CS-PCL fibrous mat for skin tissue engineering applications and hence the fibrous mats were evaluated with HaCaT in addition to standard mouse fibroblast (L-929) cell lines. HaCaT cell is non tumorigenic, genetically stable immortalized cell line from adult skin, which is used as the candidate for skin tissue engineering and is commonly used as a substitute for human keratinocyte [33]. Though a recent report on CS and PCL nanofibrous scaffold by a single step electrospinning technique has been reported, they have used osteoblast and fibroblasts for evaluating bone and skin tissue engineering applications [34]. To the authors belief this is the first report on evaluation of CS-PCL blend electrospun scaffold using keratinocytes. The CS-PCL mats favored better cell spreading, cell–cell and cell–material interaction than PCL scaffolds. The L929 and HaCaT cells seeded and cultured on both scaffolds showed good viability. However extensive patch formation, typical to skin keratinocytes was found on CS-PCL scaffolds. It is known that modifying PCL with CS improves the cell affinity and biocompatibility [35]. The polycation nature of CS in the blend fibrous mat is expected to improve serum protein adsorption than PCL thereby helps in more cell adhesion [36]. This justifies more cell adhesion on CS-PCL than PCL.

Skin tissue engineering primarily requires short in vitro manipulation time. Formation of large cell patches in CS-PCL scaffold helps in faster cell coverage thereby reducing in vitro time. The cell growth on CS-PCL measured at two time points were significantly more compared to PCL. These results are similar to previous reports with human dermal fibroblast on PCL nanofilms incorporated with CS [37]. Cell adhesion, morphology spreading, migration and ECM deposition is dependent on the distribution of actin cytoskeleton [38]. Actin cytoskeletal distribution of cells seeded on PCL and CS-PCL showed cortical staining pattern which indicates well spread morphology of cells [39]. The CS-PCL scaffolds also favored L929 cell proliferation compared to PCL indicating the blend properties of both CS and PCL. The results indicates that CS-PCL electrospun scaffolds were superior in supporting the cell proliferation compared to PCL alone and suitable for skin tissue engineering.

## 5 Conclusions

CS and PCL blend was prepared in a modified solvent of formic acid and acetone and used for electrospinning. The CS-PCL mats were evaluated for biocompatibility and its suitability for skin tissue engineering using HaCaT. The performance of the blend mats were compared with PCL mats. The CS -PCL fibrous mats showed enhanced cell

adhesion cell spreading and proliferation. Improved cell material interaction of HaCaT cells on CS-PCL suggests that blending CS with PCL makes it a better substrate for skin tissue engineering.

**Acknowledgments** The research work was supported by the DST Fast Track Grant (SR/FT/LS-128/2009, Government of India). The authors acknowledge the technical help from Mr. Arumugham V. and Ms. Leena Joseph, Calibration Cell for profilometry analysis and Ms. Geetha, Department of Tissue Engineering and Regenerative Technologies for contact angle measurements.

## References

1. Kumbar SG, Nukavarapu SP, James R, Nair LS, Laurencin CT. Electrospun poly(lactic acid-co-glycolic acid) scaffolds for skin tissue engineering. *Biomaterials*. 2008;29(30):4100–7.
2. Martins A, Araujo JV, Reis RL, Neves NM. Electrospun nanostructured scaffolds for tissue engineering applications. *Nanomedicine (Lond)*. 2007;2(6):929–42.
3. Blakeney BA, Tambralli A, Anderson JM, Andukuri A, Lim DJ, Dean DR, et al. Cell infiltration and growth in a low density, uncompressed three-dimensional electrospun nanofibrous scaffold. *Biomaterials*. 2011;32(6):1583–90.
4. Prabhakaran MP, Venugopal JR, Ramakrishna S. Mesenchymal stem cell differentiation to neuronal cells on electrospun nanofibrous substrates for nerve tissue engineering. *Biomaterials*. 2009;30(28):4996–5003.
5. Woei K, Hutmacher DW, Schantz JT, Seng C, Too HP, Chye T, et al. Evaluation of ultra-thin poly(epsilon-caprolactone) films for tissue-engineered skin. *Tissue Eng*. 2001;7(4):441–55.
6. Gupta D, Venugopal J, Prabhakaran MP, Dev VR, Low S, Choon AT, et al. Aligned and random nanofibrous substrate for the in vitro culture of Schwann cells for neural tissue engineering. *Acta Biomater*. 2009;5(7):2560–9.
7. Wang TJ, Wang IJ, Lu JN, Young TH. Novel chitosan-poly-caprolactone blends as potential scaffold and carrier for corneal endothelial transplantation. *Mol Vis*. 2012;18:255–64.
8. Jayakumar R, Prabakaran M, Nair SV, Tamura H. Novel chitin and chitosan nanofibers in biomedical applications. *Biotechnol Adv*. 2010;28(1):142–50.
9. Zubareva A, Ily'ina A, Prokhorov A, Kurek D, Efremov M, Varlamov V, et al. Characterization of protein and peptide binding to nanogels formed by differently charged chitosan derivatives. *Molecules*. 2013;18(7):7848–64.
10. Adekogbe I, Ghanem A. Fabrication and characterization of DTBP-crosslinked chitosan scaffolds for skin tissue engineering. *Biomaterials*. 2005;26(35):7241–50.
11. Singh DK, Ray AR. Biomedical applications of chitin, chitosan, and their derivatives. *J Macromol Sci Part C*. 2000;40(1):69–83.
12. Sarasam A, Madhally SV. Characterization of chitosan-poly-caprolactone blends for tissue engineering applications. *Biomaterials*. 2005;26(27):5500–8.
13. Wu L, Li H, Li S, Li X, Yuan X, Zhang Y. Composite fibrous membranes of PLGA and chitosan prepared by coelectrospinning and coaxial electrospinning. *J Biomed Mater Res A*. 2010; 92(2):563–74.
14. Ohkawa K, Cha D, Kim H, Nishida A, Yamamoto H. Electrospinning of chitosan. *Macromol Rapid Commun*. 2004;25(18):1600–5.
15. Shalumon KT, Anulekha KH, Girish CM, Prasanth R, Nair SV, Jayakumar R. Single step electrospinning of chitosan/

- poly( $\epsilon$ -caprolactone) nanofibers using formic acid/acetone solvent mixture. *Carbohydr Polym*. 2010;80(2):413–9.
16. Salgado AJ, Coutinho OP, Reis RL. Novel starch-based scaffolds for bone tissue engineering: cytotoxicity, cell culture, and protein expression. *Tissue Eng*. 2004;10(3–4):465–74.
  17. Pham QP, Sharma U, Mikos AG. Electrospinning of polymeric nanofibers for tissue engineering applications: a review. *Tissue Eng*. 2006;12(5):1197–211.
  18. Woodruff MA, Hutmacher DW. The return of a forgotten polymer—polycaprolactone in the 21st century. *Prog Polym Sci*. 2010;35(10):1217–56.
  19. Zhong X, Ji C, Chan AL, Kazarian S, Ruys A, Dehghani F. Fabrication of chitosan/poly( $\epsilon$ -caprolactone) composite hydrogels for tissue engineering applications. *J Mater Sci Mater Med*. 2011;22(2):279–88.
  20. Ratner BD, Hoffman AS, Schoen FJ, Lemons JE, editors. *Biomaterials science: an introduction to materials in medicine*. 3 ed. Engineered Natural Materials. Waltham: The Academic Press; 2013.
  21. Dash M, Chiellini F, Ottenbrite RM, Chiellini E. Chitosan—a versatile semi-synthetic polymer in biomedical applications. *Prog Polym Sci*. 2011;36(8):981–1014.
  22. Geng X, Kwon O-H, Jang J. Electrospinning of chitosan dissolved in concentrated acetic acid solution. *Biomaterials*. 2005;26(27):5427–32.
  23. Sun K, Li ZH. Preparations, properties and applications of chitosan based nanofibers fabricated by electrospinning. *Express Polym Lett*. 2011;5(4):342–61.
  24. Sangsanoh P, Supaphol P. Stability improvement of electrospun chitosan nanofibrous membranes in neutral or weak basic aqueous solutions. *Biomacromolecules*. 2006;7(10):2710–4.
  25. Zargham S, Bazgir S, Tavakoli A, Rashidi AS, Damerchely R. The effect of flow rate on morphology and deposition area of electrospun nylon 6 nanofiber. *J Eng Fibers Fabr*. 2012;7(4):42–9.
  26. Hsia HC, Nair MR, Mintz RC, Corbett SA. The fiber diameter of synthetic bioresorbable extracellular matrix influences human fibroblast morphology and fibronectin matrix assembly. *Plast Reconstr Surg*. 2011;127(6):2312–20.
  27. Zhu X, Cui W, Li X, Jin Y. Electrospun fibrous mats with high porosity as potential scaffolds for skin tissue engineering. *Biomacromolecules*. 2008;9(7):1795–801.
  28. Neves SC, Moreira Teixeira LS, Moroni L, Reis RL, Van Blijstswijk CA, Alves NM et al. Chitosan/poly( $\epsilon$ -caprolactone) blend scaffolds for cartilage repair. *Biomaterials*. 2011;32(4):1068–79.
  29. Olivieri MP, Rittle KH, Tweden KS, Loomis RE. Comparative biophysical study of adsorbed calf serum, fetal bovine serum and mussel adhesive protein films. *Biomaterials*. 1992;13(4):201–8.
  30. Liu H, Webster TJ. Nanomedicine for implants: a review of studies and necessary experimental tools. *Biomaterials*. 2007;28(2):354–69.
  31. Affandi N, Truong Y, Kyratzis I, Padhye R, Arnold L. A non-destructive method for thickness measurement of thin electrospun membranes using white light profilometry. *J Mater Sci*. 2010;45(5):1411–8.
  32. Hsin-I Chang, Wang Y. Cell responses to surface and architecture of tissue engineering scaffolds. In: Eberli D, editor. *Regenerative medicine and tissue engineering—cells and biomaterials*. INTECH; 2011.
  33. Tao K, Bai XZ, Zhang ZF, Shi JH, Hu XL, Tang CW, et al. Construction of the tissue engineering seed cell (HaCaT-EGF) and analysis of its biological characteristics. *Asian Pac J Trop Med*. 2013;6(11):893–6.
  34. Shalumon KT, Anulekha KH, Chennazhi KP, Tamura H, Nair SV, Jayakumar R. Fabrication of chitosan/poly( $\epsilon$ -caprolactone) nanofibrous scaffold for bone and skin tissue engineering. *Int J Biol Macromol*. 2011;48(4):571–6.
  35. Mei N, Chen G, Zhou P, Chen X, Shao ZZ, Pan LF, et al. Biocompatibility of Poly( $\epsilon$ -caprolactone) scaffold modified by chitosan—the fibroblasts proliferation in vitro. *J Biomater Appl*. 2005;19(4):323–39.
  36. Jeong SI, Krebs MD, Bonino CA, Samorezov JE, Khan SA, Alsberg E. Electrospun chitosan-alginate nanofibers with in situ polyelectrolyte complexation for use as tissue engineering scaffolds. *Tissue Eng Part A*. 2011;17(1–2):59–70.
  37. Chung TW, Wang YZ, Huang YY, Pan CI, Wang SS. Poly( $\epsilon$ -caprolactone) grafted with nano-structured chitosan enhances growth of human dermal fibroblasts. *Artif Organs*. 2006;30(1):35–41.
  38. Tuzlakoglu K, Santos MI, Neves N, Reis RL. Design of nano- and microfiber combined scaffolds by electrospinning of collagen onto starch-based fiber meshes: a man-made equivalent of natural extracellular matrix. *Tissue Eng Part A*. 2011;17(3–4):463–73.
  39. Pok SW, Wallace KN, Madihally SV. In vitro characterization of polycaprolactone matrices generated in aqueous media. *Acta Biomater*. 2010;6(3):1061–8.